Attenuation Compensation in ^{99m}Tc SPECT Brain Imaging: A Comparison of the Use of Attenuation Maps Derived from Transmission Versus Emission Data in Normal Scans

Robert Licho, Stephen J. Glick, Weishi Xia, Tin-Su Pan, Bill C. Penney and Michael A. King

Department of Radiology, University of Massachusetts Medical School, Worcester, Massachusetts

Brain SPECT imaging using ^{99m}Tc lipophilic tracers such as hexamethyl propyleneamine oxime (HMPAO) attempts to estimate cerebral, cerebellar and subcortical perfusion by assessing the relative amount of tracer uptake among these regions. Most commonly, comparison is made with cerebellar activity. Because the assessment of relative tracer uptake may be rendered inaccurate by photon attenuation by the nonuniform attenuation properties of the head, brain SPECT reconstructions have been compared using attenuation correction (AC) with various methods for estimating the attenuation map. **Methods:** Patients underwent ^{99m}Tc-HMPAO brain SPECT with transmission line source AC hardware. In addition to the emission dataset, emission downscatter and transmission datasets were acquired. Iterative reconstructions using three different attenuation maps were investigated. These included: (a) that obtained from transmission imaging, (b) that obtained from segmentation of a reconstruction from a lower energy Compton scatter window and (c) a slice-independent, uniform, elliptical attenuation map. No AC was also compared. **Results:** Count profiles in patients having brain perfusion SPECT scans showed a significant difference in region count estimates in the brain depending on whether AC is used as well as on the attenuation map used. Scatter-based AC is able to provide external contour detection and attenuation compensation based on that contour, whereas transmission-based AC provides external contour detection as well as internal, nonuniform attenuation estimation and AC. If one considers transmission AC to be the clinical "gold standard," non–attenuation-corrected as well as fixed-ellipsoid, uniform attenuation-corrected studies provided unreliable regional estimates of tracer activity. **Conclusion:** This study shows the significant difference in clinical brain SPECT count profiles depending on how and whether there is compensation for attenuation. Based on prior studies validating the improved quantitative accuracy of SPECT using transmission-based AC, this study suggests that clinical ^{99m}Tc brain perfusion SPECT would benefit from and, in situations demanding rigorous quantitative assessment, requires transmission-based AC. Estimating attenuation maps with scatter-based methods was the next most accurate (clinical) method tested and can be used if and when transmission imaging cannot be used.

Received Feb. 19, 1998; revision accepted Aug. 4, 1998.

For correspondence or reprints contact: Robert Licho, MD, Department of Radiology, University of Massachusetts Medical School, 55 Lake Ave. North, Worcester, MA 01655.

Key Words: brain SPECT; neuro-SPECT; brain perfusion; attenuation correction

J Nucl Med 1999; 40:456–463

It is known that body tissue causes attenuation of photons in both planar and SPECT imaging. Several well-recognized examples of systematic artifact from photon attenuation, from the breast and diaphragm, have led to limitations in diagnostic accuracy in myocardial SPECT imaging (*1,2*). As a result, there has been a practical need for correction of atttenuation artifact in this particular application. Methods to correct for photon attenuation have used a uniform estimation of the attenuation distrubution as well as a patient-specific estimation of the attenuation distribution obtained from transmission imaging. There is compelling early evidence that attenuation correction (AC) techniques do improve clinical accuracy (*3*). Studies have shown the superior accuracy of brain SPECT using transmission-based AC (*4*). The impact of attenuation in applications apart from cardiac imaging and, specifically, the effect and implications of differing attenuation in the skull, brain tissue and sinus cavities on the accuracy of estimating regional cerebral blood flow in the clinical setting are beginning to be addressed in the literature (*5–10*).

In relative regional cerebral blood flow neuro-SPECT or brain SPECT imaging using (essentially) nonredistributing radiolabeled amines, such as hexamethyl propyleneamine oxime (HMPAO) and ethyl cysteinate dimer, cerebral cortical abnormality is most often defined qualitatively, via pattern recognition, by identifying areas of hypoperfusion or hyperperfusion compared with normal controls (*11*) or based on expected symmetry where either a visual or quantitative method is used (*12,13*). Others use a more quantitative approach and, when defining abnormality a priori, define it as <60% of cerebellar (and less commonly occipital or global cortical) perfusion (*14*). But does attenuation affect the measured relative counts of the cerebellum, cerebral cortex and subcortex on which such quantitative and even

qualitative determinations are based? As Tc-radiolabeled, amine-based brain perfusion SPECT becomes increasingly reliant on quantification and its clinical and investigational use increasingly based on comparison with normal controls, an investigation of attenuation artifact and AC techniques is necessary. If there is significant attenuation artifact, then to what extent do corrected datasets differ in count profiles from uncorrected studies? Finally, does the gain from this potential correction outweigh clinical and technical constraints of imaging and set-up time, hardware expense, camera design and processing time?

Several analytical methods have been proposed to compensate for photon attenuation, assuming uniform attenuation properties of the body. Most commercial software systems include a uniform AC package, offering edge detection and manual adjustment for estimating the body outline from photopeak data using the entire study or a selected number of slices. Another approach for estimating the attenuation map of the head is to use segmentation procedures applied to a Compton scatter window (i.e., energy window lower than the photopeak) reconstruction (*8*). The advantages of estimating the attenuation map from the emission data in this manner are as follows: (a) a patient-specific attenuation map could be obtained without transmission source hardware, which is especially appealing for single-head SPECT systems; (b) camera design might not need to be constrained or made more complex by transmission-source hardware; (c) the elimination of time lost to transmission source set-up and acquisition, the latter of which in some systems is at the expense of emission acquisition time; and (d) attenuation estimates using an emission dataset avoid the risk of misregistration that might occur using transmission-based correction when the emisssion photopeak dataset and the transmission files are obtained sequentially.

The assumption of uniform attenuation in the head is questionable, because the skull, sinus cavities and head holder all have attenuation properties that are different from brain tissue. It has been shown using simulation studies that the assumption of homogeneous attenuation throughout the head can result in quantitative errors of up to 20% in certain parts of the brain (*4*). Recently, there has been much interest in estimating nonuniform attenuation maps using SPECT transmission imaging. Many transmission imaging geometries have been proposed, including a line source opposite a fanbeam collimator (*9*), a scanning line source opposite a parallel-beam collimator (*15*), multiple line sources opposite a parallel-beam collimator (*16*) as well as others. Several investigators have begun to investigate the need for AC as well as compensation methods for brain SPECT studies and have reached differing conclusions. Stodilka et al. (*17*) have conducted phantom studies and have concluded that nonuniform attenuation compensation must be performed to accurately estimate regional cerebral blood flow. Iida et al. (*18*) have studied the effects of attenuation compensation when using a technique for estimating regional cerebral blood flow from a single SPECT scan with ^{123}I. In comparing reconstructions using both uniform and nonuniform attenuation compensation methods, they noted that larger differences in regional cerebral blood flow values occurred in lower and higher slices because of airways and the thickening skull, respectively. However, they generally concluded that the loss in quantitative accuracy using uniform attenuation compensation was small.

Using the estimated attenuation map (either uniform or nonuniform), one approach to attenuation compensation is to model attenuation into an iterative reconstruction algorithm. In this report, we examine reconstructions of clinical data using the maximum likelihood expectation maximization (MLEM) algorithm with four different estimates of the attenuation map. These include the following: method 1: an attenuation map derived from transmission imaging; method 2: a slice-dependent, uniform attenuation map estimated from the reconstruction of a lower Compton energy window; method 3: a slice-independent (i.e., cylindrical), uniform attenuation map derived from the union of the head regions of all slices in method 2 described above; and method 4: no attenuation map (i.e., no attenuation compensation). Method 3 is meant to simulate the result that would be obtained by using a single elliptical region of interest (ROI) for an entire file rather than slice-specific ROIs, because this is an option on current clinical software.

MATERIALS AND METHODS

Emission SPECT studies were acquired in patients having routine clinical ^{99m}Tc-HMPAO neuro-SPECT. We also acquired transmission-source attenuation maps as well as datasets consisting of downscatter from the emission study. From the scatter dataset, we have attempted to estimate a patient-specific attenuation map that would be obtained from the transmission dataset but by using a uniform attenuation map, obviating the need for a transmission-source acquisition.

Patients having clinically indicated perfusion brain SPECT studies gave informed consent to participate in an institutional review board–approved study to evaluate the use of transmission-based attenuation compensation to potentially improve image quality. Because we were only interested in comparing different techniques within subjects, we used patients who were having clinically indicated SPECT scans. Abnormal scans were not excluded; however, the studies obtained yielded no abnormal clinical SPECT findings. Patients with any major structural cranial or intracranial abnormality were excluded. The study was conducted using a three-detector SPECT camera (Picker 3000; Picker International, Cleveland, OH) outfitted with low-energy, ultra-high-resolution fanbeam collimators. Each collimator has a 50-cm focal length. Patients were administered 25 mCi of ^{99m}Tc-HMPAO while resting with eyes and ears open in a quiet, dimly lit room. Emission data were acquired at between 60 and 90 min after injection during a 20-min period in step-and-shoot mode. Two projection image datasets were collected, one centered on the photopeak window (140 keV, 20%) and another centered on a Compton scatter window (109 keV, 30%). A 128 × 128 matrix was used for these datasets (pixel size, 3.18 mm), which were acquired over 120 angles. Immediately afterward, a transmission study was obtained using a custom-built line source containing 20 mCi ^{99m}Tc, positioned at the focal line of one of the fanbeam collimators. Transmission images

were also sampled at 128 × 128 pixels over 120 angles for 10 min. The patient was observed continuously between emission and transmission scans for possible movement that could result in misregistration. After the transmission scan, a ^{99m}Tc flood source was acquired without the patient to normalize the transmission projection images. Attenuation maps were estimated from the transmission projection data using the iterative MLEM algorithm previously described by Lange et al. (*19*) using 60 iterations.

In addition to the attenuation maps obtained with transmission imaging, attenuation maps were estimated using a segmentation procedure applied to reconstructed images of the emission data from the Compton scatter window. This segmentation method has been described by Pan et al. (*20*). Briefly, the Compton scatter window projection data are reconstructed with filtered backprojection. Then the head outline in each slice is derived from the zero-crossing of the directional derivative on the gradient magnitude in the gradient direction, followed by a connected component operation starting at the voxel with the largest gradient in the image. This segmentation procedure results in an estimate of the head surface, and a uniform attenuation coefficient of 0.15 cm^{-1} is assumed throughout the head.

To reconstruct the emission projection data, scatter correction was first performed using the dual-window scatter subtraction described by Jaszczak et al. (*21*). By performing prereconstruction scatter compensation, narrow-beam atttenuation coefficients measured with transmission imaging could be used in the iterative reconstruction algorithm. Sixty iterations of the MLEM algorithm were then performed using three different attenuation maps: (a) that obtained with transmission imaging (trans-AC); (b) that obtained using segmentation applied to the Compton scatter window reconstruction (scatter-AC); and (c) a cylindrical, uniform attenuator derived from the union of all attenuation map slices computed from the scatter-AC segmentation procedure (UAC). The use of no attenuation compensation (NC) was also tested. These four methods were compared in each of 4 patients.

To analyze the difference between methods, ROIs were drawn manually for each patient to estimate count density within the vertex of the cerebral cortex, lower (hence, outer) cerebral cortex, subcortex (thalamic nuclei) and cerebellum. Global counts were not measured directly; instead, the aforementioned regions were also averaged into an additional category, labeled "all," in each patient. Figure 1 gives examples of these ROIs in 1 typical patient.

Because of the common practice of normalizing count density in different structures throughout the brain to the cerebellum, we performed an additional experiment to better understand how attenuation and different correction techniques can affect ROI counts recorded in the cerebellum. Using the different attenuation maps obtained for each patient (i.e., trans-AC, scatter-AC and UAC), a simulated point source located within the cerebellum was projected in the transaxial plane using a ray-tracing algorithm (*22*). Using this projection data, plots were formed of total counts versus projection angle for each attenuation map. This data provide insight into how the count density in the cerebellar ROI varies between patients and when using different estimates of the attenuation map.

RESULTS

Figure 2 shows transaxial views, over three slices, of the attenuation estimates obtained using trans-AC, scatter-AC and UAC. The top row shows how the trans-AC estimate accounts for both the body contour as well as the internal variation in attenuation, with the latter most evidently observed in the frontal sinuses. The scatter-AC file appears to contour the body but, being a uniform estimate, does not account for variable attenuation. The bottom row shows the UAC file, formed from the detected edge from the union of all transaxial slices, which results in a single transaxial external contour along the entire z-axis or a quasi-"cylinder."

We chose to perform our comparison in 4 patients to examine whether potential differences in AC were systematic or patient specific. The different patterns of corrected brain uptake in 1 of these patients using methods 1–4 are shown in Figure 3. In Figures 4A–D, the count estimates in five different brain regions using the four different ap-

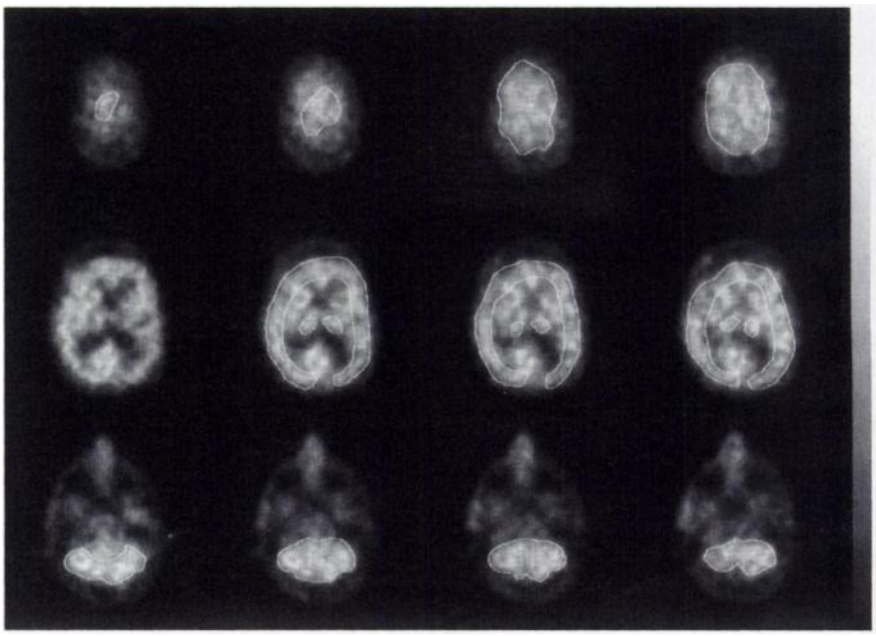

FIGURE 1. Illustration of ROIs defined for measurements of regional brain activity used for generation of plots in Figure 4A–D in 1 of 4 patients studied. Top row = vertex; middle row = cortex and nuclei; bottom row = cerebellum.

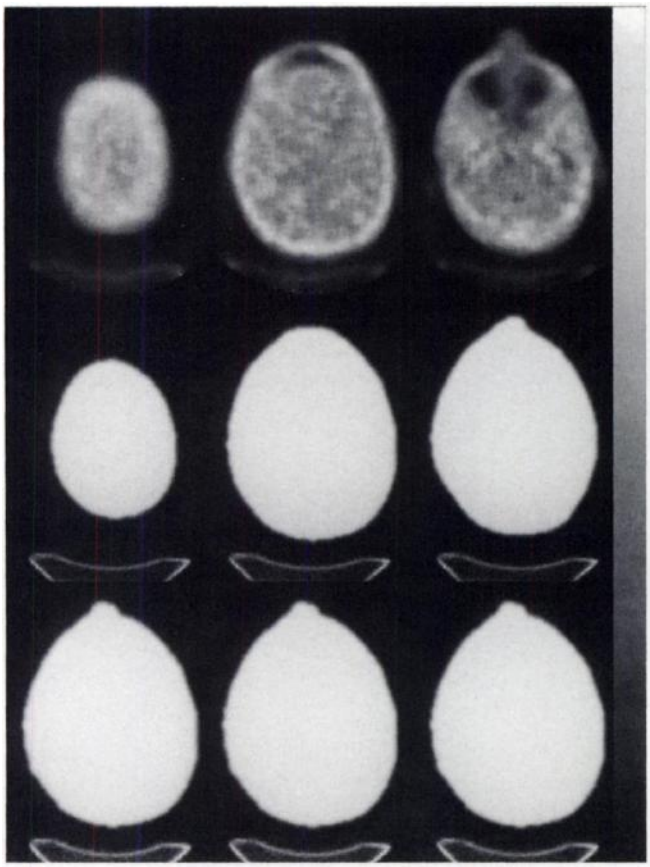

FIGURE 2. Transaxial maps over three nonconsecutive slices (from near the vertex to near the base) of the attenuation estimates obtained using trans-AC, scatter-AC and UAC. Top row shows how trans-AC estimate accounts for both body contour as well as internal variation in attenuation; latter most evidently can be seen in frontal sinuses. Scatter-AC images (middle row) appear to contour body but, being uniform estimates, do not account for variable attenuation. UAC images (bottom row) show single transaxial external contour along entire z-axis or quasi-"cylinder."

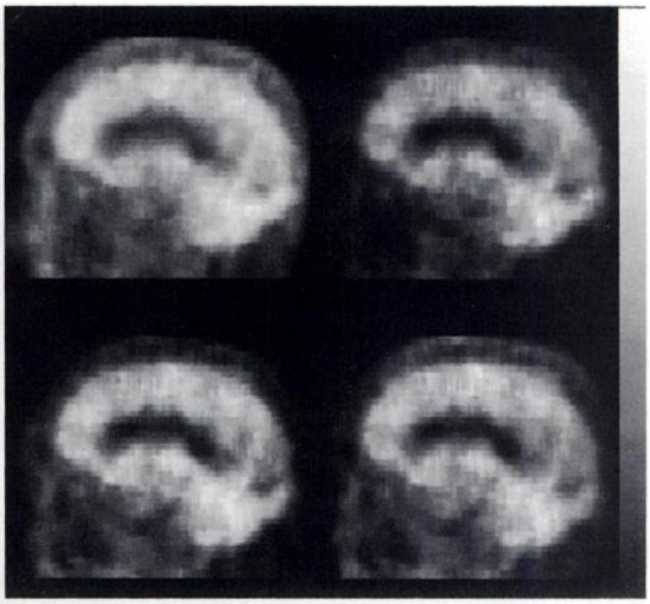

FIGURE 3. Sagittal views of 1 patient showing subtle differences in tracer distribution patterns that resulted from different approaches to attenuation. Clockwise from top left: no correction, trans-AC, UAC and scatter-AC. Note low thalamus/cortex ratio in no correction compared with all other images. Also note in trans-AC (appropriately) low signal in frontal sinus as well as oropharyngeal region, which includes in part maxillary sinuses, all of which are air containing. Lastly, note higher counts in vertex in UAC compared with all others.

proaches to attenuation compensation are plotted against each other in each of the 4 patients tested (A–D).

All correction techniques increased the absolute count estimates between 2- and 2.5-fold throughout the brain compared with SPECT with no correction. In Figure 4A–D, the absolute count estimates using these different techniques are normalized to each other. The global count estimates resultant from all of the correction techniques were similar; this is depicted by the "all" category in Figure 4A–D, which represents the average of the different ROIs in the brains of patients 1–4. However, significant differences in count profiles within the brain (i.e., among different regions and/or structures within brains) were observed between corrected and uncorrected images as well as among the different AC techniques. Several of these differences were observed consistently in all subjects studied; other differences were subject specific.

Uncorrected studies of all subjects showed lower counts in the nuclei (thalami) than in the outer cortex, but when corrected with trans-AC, scatter-AC or UAC showed an increase in thalamus/cortex ratio and, with one exception, showed higher counts in the nuclei than in the cortex. This is visually appreciable in Figure 3. In addition, there was, however, a significant difference in the thalamus/cortex ratio depending on the method of correction used. Both the scatter-AC and UAC methods consistently gave a higher thalamus/cortex ratio compared with trans-AC correction. This finding is possibly a reflection of a secondary effect of peripheral attenuation by the skull having a greater attenuation effect on the outer cortex immediately adjacent to it. When this nonuniform attenuator is accounted for by transmission correction, a greater compensation results in the outer cortex relative to the center of the brain, as opposed to when the skull is not considered. This difference was less pronounced in patient 3 compared with patients 1, 2 and 4. To explain this difference, point-source studies were performed on patients 1 and 3 in which a theoretical point source positioned at the center of the cerebellum was projected using ray tracing through each of the attenuation maps used. Plots were then formed of total counts versus projection angle for each attenuator (Fig. 5). These plots were compared and showed differing amounts of attenuation depending on the particular shape and content of each skull, with the most conspicuous difference being in the count estimate in the posterior 120°, which was higher in patient 3.

In patient 3, there was also a marked overestimation of cerebellar counts in UAC and scatter-AC (relative to trans-

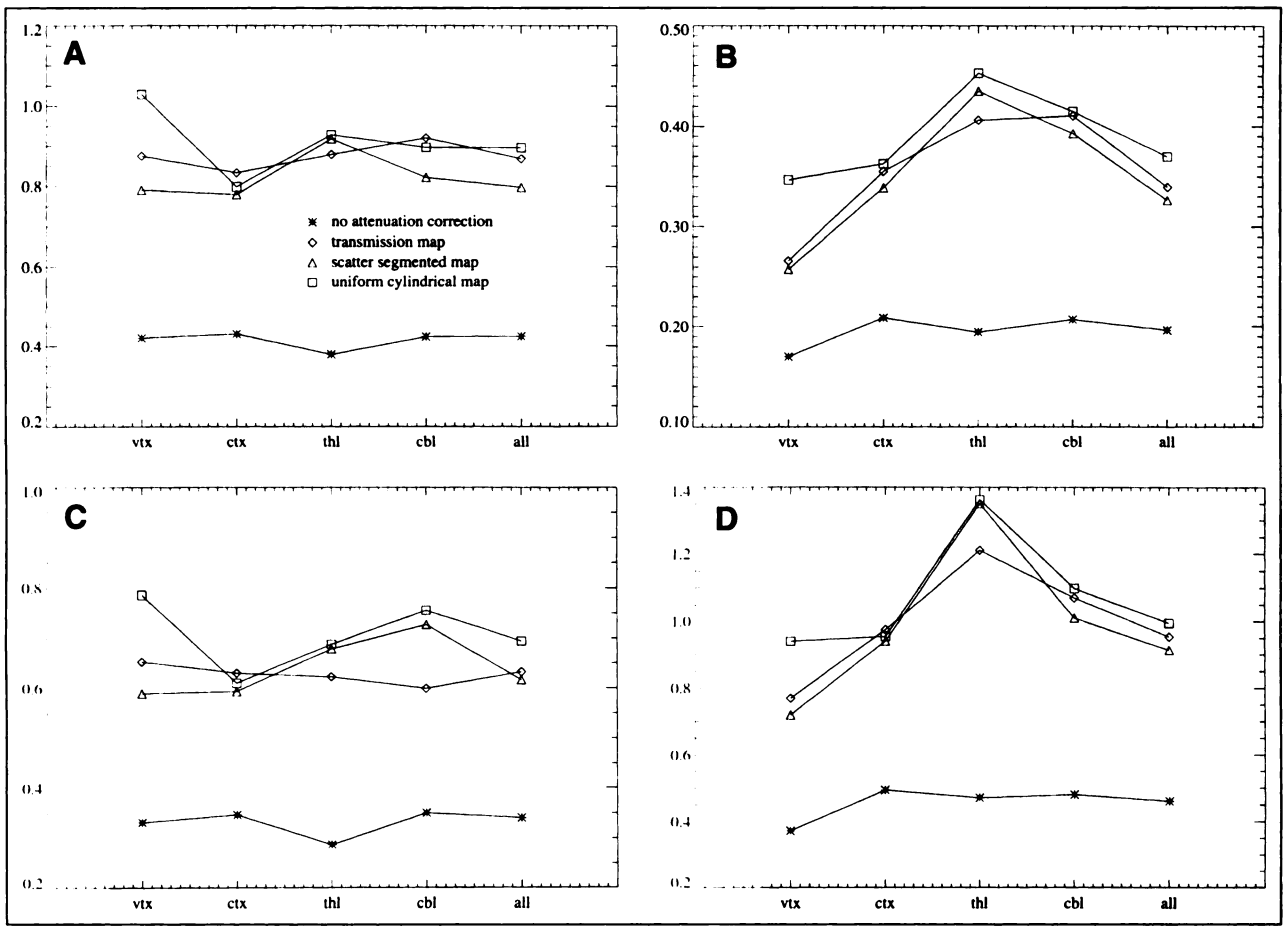

FIGURE 4. Count estimates in five different brain regions using the four different approaches to attenuation compensation. (A) patient 1, (B) patient 2, (C) patient 3 and (D) patient 4. ◇, trans-AC; △, scatter-AC; □, UAC; ∗, no correction.

AC, by approximately 20%). UAC and scatter-AC of patients 1, 2 and 4 showed variable overestimation and underestimation of the cerebellum, raising the question of nonuniform or nonsystematic factors in producing errors of cerebellar count estimates. This was again addressed by point-source studies in patients 1 and 3 (Fig. 5A and B). These plots were compared and showed differing degrees of attenuation depending on the particular shape and content of each skull. Differences noted that might have contributed to the differing attenuation included the thickness of the skull

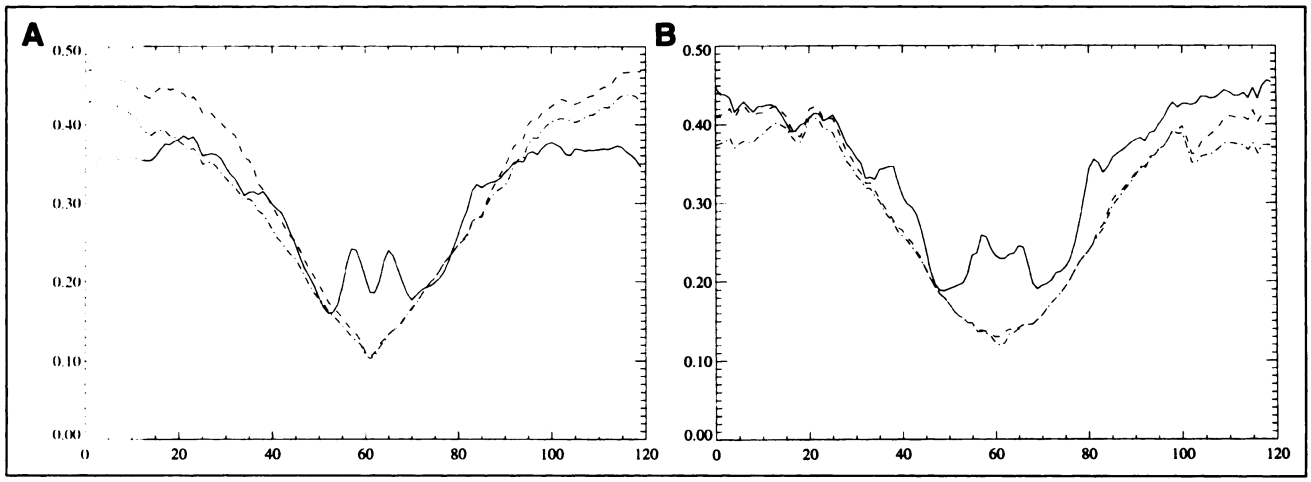

FIGURE 5. Simulated point source located within cerebellum was projected in transaxial plane using ray-tracing algorithm (*15*) in patients 1 (A) and 3 (B). Plots were formed of total counts versus projection angle using each attenuation map. ——, Transmission map; – –, scatter-AC map; – - –, UAC map.

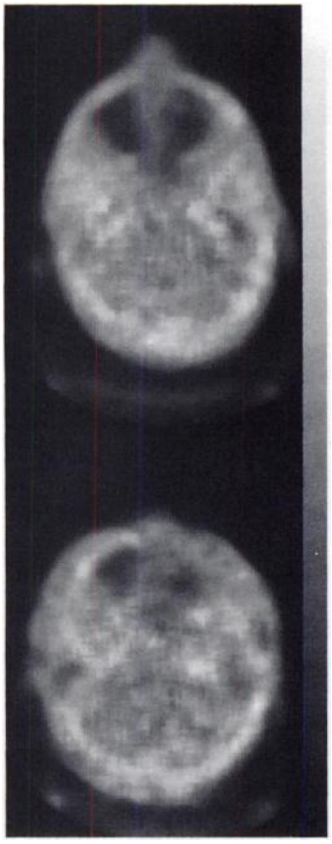

FIGURE 6. Transaxial attenuation images of patients 1 and 3 that were used to generate images in Figure 5. Note differences in skull shape and sinus size and density.

relative to its roundness as well as the size and shape of the sinuses (Fig. 6). These findings helped to show the differences in variable attenuation between individual subjects and how this variation can change the relative cerebellar count estimate.

In all subjects, the UAC method over-corrected vertex counts, that is, showed consistently higher relative counts in the vertex compared with trans-AC and to a significant degree (Fig. 4). Scatter-AC, on the other hand, consistently provided lower relative vertex counts compared with trans-AC, although this difference was relatively small.

DISCUSSION

Impact of Attenuation and Relative Value of Different Attenuation Correction Methods

Previous studies using simulation data have validated the accuracy of transmission-based attenuation compensation in improving count profiles within the brain (*4*). Based on this assumption, we chose to use trans-AC as our gold standard for this in vivo evaluation of commonly available AC methods, which in some clinical settings includes no correction at all.

Our data suggest that there are both systematic as well as patient-specific differences between the methods tested. Any of the three forms of AC tested improve estimates of count profiles within the cerebrum, with all methods increasing subcortical count estimates. Achieving an accurate circumferential boundary estimate, i.e., by scatter-AC, was sufficient for correctly estimating the relative count profile between the outer cortex, subcortex (i.e., nuclei) and vertex. This was not possible using UAC, with the overestimation of vertex counts being attributable to the overestimation of the head radius in these slices by the cylindrical nature of the attenuation dataset. None of the uniform correction methods performed similarly to transmission correction in estimating the correct count profiles between regions of the cerebral cortex and the cerebellum. This finding is significant given the use of relative cerebellar counts in the interpretation of ethyl cysteinate dimer/HMPAO neuro-SPECT studies. In addition to detecting the increased attenuation from the skull, regional increased attenuation can also be detected using trans-AC, perhaps from asymmetric skull density, differing skull shapes and thicknesses and differing sinus sizes and densities, which in turn can affect local count estimates, including the cerebellar count estimate. Primarily for this reason, we believe that transmission-based AC should be used in brain SPECT imaging and is mandated by quantitative SPECT. (It would be useful to evaluate the potential benefit of using trans-AC in SPECT patients who have had partial craniectomy.)

Control Data from Healthy Individuals

Before trans-AC can be used clinically, the count profile of healthy individuals needs to be known. For example, bilateral alterations of the subcortex/cortex ratio are observed in degenerative dementias and movement disorders and bilateral traumatic shear injury. Asymmetric alterations in the subcortex/cortex ratio are observed in subcortical infarcts and traumatic shear injury. Quantitative results have also been reported for the cortex and subcortex in fibromyalgia (compared with healthy controls) using Chang AC (*23*), and such numbers could be expected to differ, in both healthy controls and test subjects, using trans-AC or NC. Hence, although AC can provide more accurate subcortical count estimates, a trans-AC control database ultimately needs to be available to properly interpret these studies. Until such a database is collected, it may be necessary to reconstruct neuro-SPECT studies both with and without trans-AC, using non-AC healthy control data with the uncorrected file.

In the absence of absolute quantification of cerebral blood flow using ^{99m}Tc-based amines, the cerebellum is typically used for reference. Although this method leaves concern regarding the accuracy of assuming normal cerebellar perfusion, it is anticipated that attenuation-corrected control databases will provide information regarding the normal range of cerebral activity versus cerebellar activity, which is at least not influenced by anatomy, i.e., subject to attenuation artifact from sinus size, skull shape and thickness and the like. Thus, although not providing absolute quantification, AC can offer improved accuracy in the semiquantitation that is clinically available using these agents.

Practical and Technical Feasibility of Attenuation Correction

Other than the line-source hardware requirement of trans-AC, acquisition of trans-AC and scatter-AC are similar in that they require collection of additional datasets that can be included in a predefined acquisition protocol. Once these files are acquired and selected, transverse reconstruction and AC of these studies is entirely operator independent and requires fewer than 20 min of computation time using an alphastation 400 with a 233-MHz processor. Postfiltering, magnification and orthogonal reorientation and/or reconstruction are then performed by standard technique. (In our clinic, this includes choosing filter parameters that are optimized for the statistical quality of the individual study, which can vary not just by imaging radius and dose but also by total brain counts acquired.) Hence, because the trans-AC and scatter-AC techniques do not require interactive contouring, processing using these methods is actually less labor intensive and operator dependent than conventional Chang-type AC, in which it is usually necessary to manually override, slice by slice, the edge-detected photopeak body contour.

At times, transmission AC is not possible. This can be because of the unavailability of technology in a given locale or because of logistical limitations of performing trans-AC. Examples of the latter include excessive patient size (large body and short neck), which can actually result in a collision between the patient and the transmission source or even a collision between the patient and the detector, the position of which may be limited by the requirements of the transmission hardware. Such circumstances may be ones in which the scatter-AC method may prove useful for improving, if only partially, the accuracy of these SPECT studies.

To date, conventional SPECT imaging software has used manually drawn or edge detection–generated ellipses (or a combination of both) generated from the ^{99m}Tc emission photopeak reconstructed image. We used scatter windows to compare MLEM-based AC using uniform slice-by-slice body contours (scatter-AC) with that using a uniform single contour, cylindrical along the z-axis (UAC). We did not hypothesize or test for a difference in results between the use of a scatter window for boundary determination versus the use of the ^{99m}Tc photopeak window for this purpose. We found the scatter-AC technique to be effective in correctly detecting the patient boundary, with special attention to slices where there was considerable nonbrain tissue attenuator within the slice, such as mandibular, maxillary and sinus structures in the lower slices containing the cerebellum. This technique did not require manual boundary placement or override. We did not evaluate whether photopeak-based automatic or manually overriden boundary detection is as effective, but we expect that if it is, the results would be equivalent to those of scatter-AC. The possibility exists, however, that photopeak-based AC may not be as accurate in detecting the nonbrain tissue boundary as scatter-AC, in which the scatter photons in question are produced to a large extent by this tissue.

Possible Trade-off Between Count Profile Accuracy and Resolution

We used a custom line-source holder built in our own institution that, with our 50-cm focal line fanbeam collimator, afforded an imaging radius of between 14.5 and 15 cm. However, in the absence of line-source hardware, a radius of 14 cm is typically possible in clinical practice. We therefore estimate that in accommodating the radius dictated by the trans-AC hardware and geometry, there was a loss of, on average, between 0.5- and 1-cm radius. It should be noted that the commercially available Picker simultaneous transmission-emission protocol system, with its particular fanbeam collimator focal length and the displacement of the Picker simultaneous transmission-emission protocol line-source holder, necessitates an imaging radius of 15.9 cm, resulting in further loss of imaging radius. This constraint raises the question of whether the increase in count profile accuracy from commercially available trans-AC will be offset by a significant loss of resolution. Although the fall-off of resolution with imaging radius with the fanbeam collimation used in the Picker system is comparatively slow, this problem is still of moderate concern to the extent that at our center we would prefer to use our home-built system. We would suggest an eventual upgrading of the simultaneous transmission-emission protocol and other similar hardware such that it enables optimal brain imaging with an imaging radius of as small as 14 cm, thereby maximizing both resolution and count profile accuracy.

Need for Scatter Correction

Prereconstruction scatter compensation was performed in all cases for two reasons. Our transmission imaging technique produces an estimate of the narrow-beam attenuation coefficient map. Therefore, to accurately apply attenuation compensation with iterative reconstruction, scatter must first be removed from the projection data (by removing or reducing scatter before reconstruction, the assumption of narrow-beam geometry is more accurate). Second, we believe that both scatter and attenuation compensation must be performed to limit image artifacts. One example of this phenomena has been discussed in cardiac imaging (*24,25*), where scatter emanating from a hot liver can introduce artifacts into the inferior wall. For these reasons, we believe that comparing attenuation compensation methods without prior scatter correction could yield misleading results.

CONCLUSION

Based on simulation studies that have shown that trans-AC can accurately correct for nonuniform attenuation, we have compared various alternatives to trans-AC to determine whether they have comparable accuracy for clinical use. All forms of AC tested were capable of reasonable correction of count estimates of the subcortex, and scatter-AC was reasonably adequate for estimating the relative count estimates within the entire cortex and subcortex. Nonuniform attenuation, however, was found to produce an unpredict-

able variation in cerebellar count estimates, which could not be corrected by uniform AC methods. This poses a significant problem clinically, given the use of healthy control relative cerebellar count ratios for clinical neuro-SPECT interpretations. We therefore conclude that trans-AC should ideally be used in neuro-SPECT imaging to improve accuracy and statistical strength in interpreting these studies. This also necessitates development of a trans-AC healthy control database as well as further, albeit minor, optimization of existing trans-AC geometry and hardware.

When transmission AC is either not available or not logistically feasible, a method to accurately estimate external contour, such as the scatter-AC method previously described, provides a significant improvement in count estimation relative to either no AC or a single transaxial contour estimate.

ACKNOWLEDGMENTS

This study was presented in part at the 1994 annual meeting of the Society of Nuclear Medicine. This study was supported by grant NS-32323 from the National Institute of Neurological Disorders and Stroke. Its contents are solely the responsibility of the authors and do not necessarily represent the official views of the National Institute of Neurological Disorders and Stroke.

REFERENCES

1. Datz FL, Gullberg GT, Zeng GL, et al. Application of convergent-beam collimation and simultaneous transmission emission tomography to cardiac single-photon emission computed tomography. *Semin Nucl Med.* 1994;24:17–37
2. DePuey EG, Garcia EV. Optimal specificity of thallium-201 SPECT through recognition of imaging artifacts. *J Nucl Med.* 1989;30:441–449.
3. Ficaro EP, Fessler JA, Shreve PD, Kritzman JN, Rose PA, Corbett JR. Simultaneous transmission/emission myocardial perfusion tomography. *Circulation.* 1996;93:463–473.
4. Glick SJ, King MA, Pan TS, Soares EJ. Compensation for nonuniform attenuation in SPECT brain Imaging. *IEEE Trans Nucl Sci.* 1996;43:737–750.
5. Kemp BJ, Prato FS, Dean GW, Nicholson RL, Reese L. Correction for attenuation in technetium-99m-HMPAO SPECT brain imaging. *J Nucl Med.* 1992;33:1875–1880.
6. Turkington TG, Gilland DR, Smith MF, Greer KL, Jaszczak RJ, Coleman RE. A direct measurement of skull attenuation for quantitative SPECT. *IEEE Trans Nucl Sci.* 1993;40:1158–1161.
7. Zhang JJ, Park CH, Kim SM, Intenzo C, Reyes P. The attenuation effect in brain SPECT. *Clin Nucl Med.* 1993;18:583–586.
8. Pan TS, Licho R, Penney BC, Rajeevan N, Glick SJ, King MA. Attenuationcompensation in Tc99m SPECT brain imaging: use of attenuation maps derived from transmission versus emission data [abstract]. *J Nucl Med.* 1994;35:193P.
9. Kemp BJ, Prato FS, Nicholson RL, Reese L. Transmission computed tomography imaging of the head with a SPECT system and a collimated line source. *J Nucl Med.* 1995;36:328–335.
10. Hashimoto J, Kubo A, Ogawa K, et al. Scatter and attenuation correction in technetium-99m brain SPECT. *J Nucl Med.* 1997;38:157–162.
11. Tatum WO, Alavi A, Stecker MM. Technetium-99m-HMPAO SPECT in partial status epilepticus. *J Nucl Med.* 1994;35:1087–1094.
12. Rowe C, Berkovic SF, Sia STB, et al. Localization of epileptic foci with postictal single photon emission computed tomography. *Ann Neurol.* 1989;26:660–668.
13. Duncan R, Patterson J, Roberts R, et al. Ictal/postictal SPECT in the presurgical localisation of complex partial seizures. *J Neurol Neurosurg Psychiatry.* 1993;56: 141–148.
14. Holman BL, Johnson KA, Gerada B, Carvalho PA, Satlin A. The scintigraphic appearance of Alzheimer's disease: a prospective study using technetium-99m-HMPAO SPECT. *J Nucl Med.* 1992;33:181–185.
15. Tan P, Bailey DL, Hutton BF, et al. A moving line source for simultaneous transmission/emission SPECT [abstract]. *J Nucl Med.* 1989;30:964P.
16. Cellar A, Sitek A, Harrop R. Reconstruction of multiple line source attenuation maps. *Conf Proc IEEE Nucl Sci Symposium.* 1996;1420–1424.
17. Stodilka RZ, Kemp BJ, Prato FS, Nicholson RL. Importance of bone attenuation in brain SPECT quantification. *J Nucl Med.* 1998;39:190–197.
18. Iida H, Narita Y, Kado H, et al. Effects of scatter and attenuation correction on quantitative assessment of regional blood flow with SPECT. *J Nucl Med.* 1998;39:181–189.
19. Lange K, Bahn M, Little R. A theoretical study of some maximum likelihood algorithms for emission and transmission tomography. *IEEE Trans Med Imaging.* 1987;6:106–114.
20. Pan TS, King MA, deVries DJ, Ljungberg M. Segmentation of the body and lungs from Compton scatter and photopeak window images in SPECT: a Monte Carlo investigation. *IEEE Trans Med Imaging.* 1996;15:13–24. [Correction published in 1996;15:394–396.]
21. Jaszczak RJ, Greer KL, Floyd CE, Harris CC, Coleman RE. Improved SPECT quantification using compensation for scattered photons. *J Nucl Med.* 1984;25:893–900.
22. Siddon RL. Fast calculation of the exact radiological path for a three-dimensional CT array. *Med Phys.* 1985;12:252–255.
23. Mountz JM, Bradley LA, Modell JG, et al. Fibromyalgia in women: abnormalities of regional cerebral blood flow in the thalamus and the caudate nucleus are associated with low pain threshold levels. *Arthritis Rheum.* 1995;38:926–938.
24. Nuyts J, Dupont P, den Maegderbergh VV, et al. A study of the liver-heart artifact in emission tomography. *J Nucl Med.* 1995;36:133–139.
25. Germano G, Chua T, Kiat H, et al. A quantitative phantom analysis of artifacts due to hepatic activity in technetium-99m myocardial perfusion SPECT studies. *J Nucl Med.* 1994;35:356–359.